BIOLOGY OF REPRODUCTION **59,** 84–92 (1998)

Developmental Schedule of the Postnatal Rat Testis Determined by Flow Cytometry[1]

Mira Malkov, Yonit Fisher, and Jeremy Don[2]

Department of Life Sciences, Bar-Ilan University, Ramat-Gan 52900, Israel

ABSTRACT

Analysis of the biochemical events and the genes expressed at various postnatal developmental stages in the testis of mammals is of great importance for understanding spermatogenesis in general and meiosis in particular. A prerequisite for such an analysis is the characterization of a detailed developmental schedule of the postnatal testis. In this study we used four-parameter flow cytometry analysis to determine a detailed testicular developmental schedule in rats as compared to mice. A dot plot of forward-scatter/side-scatter of testicular cell suspensions from mature animals revealed 7 distinct subpopulations within the testis. These, when analyzed by fluorescence parameters, were divided into 4 levels of fluorescence: cells containing 4d DNA, 2d DNA, and 2 levels of haploid cells. Observing the acquisition pattern of these subpopulations during postnatal development, we were able to suggest the following developmental schedule for the rat. At postnatal Days 6–7, the testis contains somatic cells and spermatogonia cells only. By Days 13–14, leptotene spermatocytes appear; by Days 17–18, zygotene spermatocytes are present; by Days 19–20 and Days 22–23, early and late pachytene spermatocytes, respectively, are seen. Haploid round spermatids first appear at Days 24–25 and elongating spermatids by Days 30–31; by Day 36, elongated spermatozoa can be found.

INTRODUCTION

Mammalian spermatogenesis, the process of male gamete production, can be divided into 2 phases: 1) a prenatal phase that basically consists of male sex determination and testicular organogenesis and 2) a postnatal phase during which spermatogonial stem cells differentiate into mature spermatozoa. During the prenatal phase (for review, see [1]), primordial germinal cells translocate from the yolk sac, their site of origin, to the hindgut. From there they migrate to and colonize the gonadal ridges, which are composed of coelomic epithelial cells and mesonephric mesenchymal cells. After several mitotic cycles, these primordial germinal cells (now gonocytes, the spermatogonial precursors) and the coelomic epithelium-derived cells (now Sertoli cell precursors) aggregate, become surrounded by a basal lamina, and fuse with each other to form the testicular cords. The mesonephric mesenchymal-derived cells (now precursors of Leydig cells and peritubular cells) are excluded from the testicular cords. Correlated with the formation of the testicular cords, the SRY DNA-binding protein (encoded by the chromosome Y-specific *sry* gene) activates the MIS (Müllerian inhibiting substance) gene expression in Sertoli precursors while inactivating the cytochrome P_{450} aromatase gene expression in the Leydig cell precursors [2]. The MIS leads to regression of the female's Müllerian ducts, and inactivation of the cytochrome P_{450} aromatase prevents the conversion of testosterone to estradiol; thus testosterone is available to participate in the formation of the male's wolffian ducts and determination of the individual's male phenotype.

The postnatal phase can be divided into three main stages: 1) mitotic proliferation of spermatogonial stem cells and premeiotic differentiation of spermatogonia cells to diploid primary spermatocytes; 2) meiotic differentiation of primary spermatocytes to haploid early round spermatids via two successive divisions—the reductional division, in which homologous chromosomes are separated into two haploid secondary spermatocytes (each chromosome consists of two chromatids), and an equational division in which the two chromatids of each chromosome are separated into two haploid round spermatids; and 3) spermiogenesis, a cellular and nuclear reorganization process that turns spermatids into spermatozoa [3]. This latter stage consists of intensive condensation of the chromatin due to replacement of histones by transition proteins and later by protamines [4–7], a substantial reduction in the cell's volume due to severance of large cytoplasmic fragments, the residual bodies, and formation of a compact head and a long tail.

Although the structural and morphological characteristics of spermatogenesis are well defined, very little is known about the molecular regulation of this key biological process. A major limitation in the study of genes and factors involved in germ cell differentiation has been the lack of an efficient in vitro system that supports this differentiative process. A partial alternative to use of the in vitro system was to study the transcription and protein expression pattern of various genes in isolated populations of spermatogenic cells derived from adult testes. Testicular cell suspensions were separated by velocity sedimentation at unit gravity or by centrifugal elutriation. However, only three main populations of cells could be obtained using this technique: meiotic prophase spermatocytes (predominantly in the pachytene stage of meiosis), postmeiotic early spermatids, and elongated spermatids. An additional fraction of residual bodies and cytoplasmic fragments could also be obtained [8–10]. Flow cytometry of testicular cell suspensions was utilized as another useful tool for studying mammalian spermatogenesis. Various fluorescent dyes were used to stain DNA (and/or other components) of testicular cells, and the stained cells were analyzed or sorted according to the intensity of fluorescence emission, which correlates with DNA content [11–19]. This technique has also been used as a diagnostic tool to assess spermatogenesis as well as development of testicular cancer in human patients [20–22]. However, since the adult testis consists of cells at all stages of spermatogenic differentiation, the approaches mentioned above cannot enable accurate analysis of stage-specific biochemical events and gene expression. An efficient way to address this problem is to analyze the biochemical events and gene expression in postnatal testes following testicular development and germ cell differentiation.

Accepted February 19, 1998.
Received June 3, 1997.
[1]This research was supported by the Israel Science Foundation administered by the Israel Academy of Sciences and Humanities.
[2]Correspondence. FAX: 972-3-5351824; e-mail: don@ashur.cc.biu.ac.il

This approach, however, requires a detailed predetermination of the testicular developmental schedule. Bellve et al. [23] have determined a developmental timetable in CD-1 mice by separating seminiferous epithelial cells from testes of animals at different postnatal ages, using the sedimentation velocity at unit gravity method, and analyzing them morphologically by electron microscopy. However, although the rat is widely used as a model system for studying spermatogenesis in mammals, only partial information on spermatogenesis in rat during testicular development is available [11, 24]. A detailed developmental schedule has not been characterized.

In this study we used four-parameter flow cytometry to determine the rat's testicular developmental schedule as compared to that of the mouse. This developmental schedule, together with the advantage of efficiently separating the testicular cell subpopulations using the FACS (fluorescence-activating cell sorter) machine, will enable an easy and accurate analysis of the developmental stage-specific biochemical events and gene expression in the rat as well as the mouse.

MATERIALS AND METHODS

Source of Tissues

Balb/C mice, older than 60 days, and Sprague-Dawley rats, older than 80 days, were used as a source of normal adult tissues for all experiments. For the developmental studies, neonatal testes were collected from animals at Days 5–31 and Days 5–60 of postnatal development of mice and rats, respectively. Day of delivery was designated Day 1. Litter size was adjusted to a maximum of 8 pups per mother for the mice and 10 for the rats. Animals were killed by cervical dislocation. Large animals were killed with chloroform prior to dissection. This investigation was conducted in accordance with the Guiding Principles for the Care and Use of Research Animals Promulgated by the Society for the Study of Reproduction.

Preparation of Testicular Cells

Testes were dissected into a petri dish containing ice-cold sterile separation medium (4 mM L-glutamine, 1.5 mM sodium pyruvate, 10% fetal calf serum, and 75 μg/ml ampicillin in Dulbecco's Modified Eagle's medium containing nonessential amino acids). For each experiment with a given developmental stage, testes from several animals (4–6 pups among early postnatal animals down to 2 mature animals) were pooled and processed. Each testis was decapsulated by making a small incision in the testis and forcing (by sterile tweezers) the content of the testis through the incision into a 15-ml Falcon (Los Angeles, CA) tube containing 5 ml ice-cold separation medium. Then, 0.25 ml collagenase (Calbiochem-Behring, La Jolla, CA) from a 2 mg/ml stock solution (prepared in separation medium) was added to the tube with the decapsulated testes, and incubation was carried out for 5 min at 35–37°C under vigorous shaking. The seminiferous cords were then allowed to sediment to the bottom of the tube while being incubated on ice. The seminiferous cords were washed twice in 10 ml separation medium, resuspended in 12 ml separation medium containing 2.5 μg/ml trypsin and 1 U/ml DNase I (Boehringer Mannheim, Mannheim, Germany), incubated for 2 min at 35–37°C, and transferred to ice. Using a pasteur pipette, the seminiferous cords were disintegrated into single cells and were then filtered through a 50-μm nylon mesh, washed twice with separation medium (centrifugation at 200–300 $\times$ *g*), and counted. Experiments with the various developmental stages were repeated at least three times (using a pool of testes at the specific developmental stage in each experiment, as mentioned above).

FACS Analysis

For FACS analysis, testicular cells were brought to a concentration of 2×10^6 cells/ml in separation medium and diluted 1:1 with propidium iodide solution (10 mM Tris pH 8, 1 mM NaCl, 0.1% Nonidet P-40, 0.7 mg/ml RNase A, and 0.05 mg/ml propidium iodide). Cells were analyzed by a Becton, Dickinson (Rutherford, NJ) FACSort instrument, equipped with an argon laser, within 2 h from staining. Excitation was at 488 nm and emission at 585 nm. Four parameters were measured for each cell: forward scatter (FSC-H); side scatter (SSC-H); total fluorescence emitted from the cell (FL2-A); and the duration of emitted fluorescence from the cell (FL2-W), which correlates to the nucleus diameter. For microscopic analysis, cells from designated populations were sorted into a tube containing 1 ml separation medium, washed (3 times) in PBS, and applied onto 3-aminopropyltriethoxy-silane-treated slides. The cells were then fixed with 4% paraformaldehyde (30 min), washed (3 times) with PBS, and stained with hematoxylin.

RESULTS

For each experiment, the results are represented by three windows. The first window (illustrated in Fig. 1, a and b and Fig. 2, a and b) depicts FSC-H, which roughly represents the cell's size, plotted against SSC-H, which represents the granularity of the cell. The second window (illustrated in Figs. 1c and 2c) depicts FL2-A plotted against FL2-W. The third window (illustrated in Figs. 1d and 2d) is a histogram that represents the number of cells at each fluorescence level (FL2-A). Distinct cell populations in the first window were gated and designated R1–R8 in order to enable tracing of these cells in the second window and determination of their fluorescence level. Since all testicular cell types are contained within the mature testis, we first determined the testicular cell subpopulations in the mature testis of both the mouse and rat. Seven distinct subpopulations (R1–R7) were consistently identified in both mouse and rat testes (Fig. 1, a and b and Fig. 2, a and b). An additional group (R8), which localized to the origin of axes in all experiments performed in this study, was identified as cell debris and therefore omitted from all figures. Using a different color to present each subpopulation in the second window, we were able to divide the cells into four major fluorescence levels: the highest level with fluorescence intensity twice the intensity of the second level, the second with fluorescence intensity twice that of the third, and a fourth level that represents variable fluorescence intensities all of which are lower than that at the third level (Fig. 1, c and d and Fig. 2, c and d). R1 and R2, the largest cells (highest FSC-H levels) differing by their SSC-H values, compose the highest fluorescence level, with R2 having slightly higher FL2-W values (Figs. 1c and 2c). These cells contain 4d DNA, meaning that they are either in the G2 phase of a mitotic cell cycle or in the prophase I stage of the meiotic division. However, since the somatic cells do not proliferate in the mature testis [25, 26] and the portion of spermatogonia cells undergoing mitotic divisions is very small [27], the R1 and R2 cells must represent primary

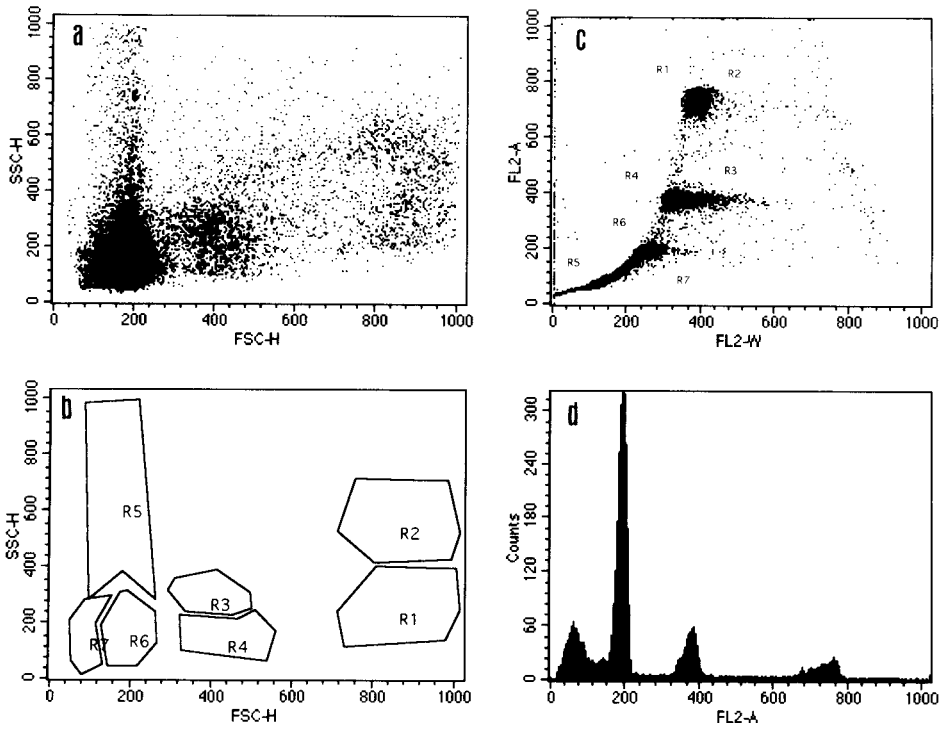

FIG. 1. FACS analysis of a testicular cell suspension obtained from an adult mouse. **a**) First window, in which cells are distributed according to size (FSC-H) and cellular granularity (SSC-H). **b**) The frame of the first window overlaid with marks representing the seven gated groups. Marks are not shown on original plot to enable better discrimination of the groups mentioned. **c**) Second window, in which cells are distributed according to fluorescence intensity (FL2-A) and width of the emitted fluorescence (FL2-W). Location of gated groups is marked by their group number (R1-R7). **d**) A histogram that represents the number of cells at each fluorescence level.

spermatocytes at prophase I of the meiotic division. Indeed, microscopic examination revealed that isolated R1 and R2 cells exhibited different stages of meiotic chromatin organization. Nuclei of R2 cells were less compact then R1 nuclei (larger diameter—consistent with higher FL2-W values), and the meiotic chromosomes were apparent (Fig. 3, b and c). R3 and R4 are the 2d cells, consisting mainly of testicular somatic cells (Sertoli, Leydig, and peritubular cells), but also of spermatogonia at the G1 phase of the cell cycle, preleptotene spermatocytes prior to the premeiotic S phase, and secondary spermatocytes between the two meiotic divisions. FL2-W values were slightly elevated for the R3 cells as compared to the R4 cells. R5–7 represent three haploid subpopulations. R6 are early round spermatids, with FL2-A values of around channel 200 (Fig. 1, c and d and Fig. 2, c and d). Elongating spermatids were localized

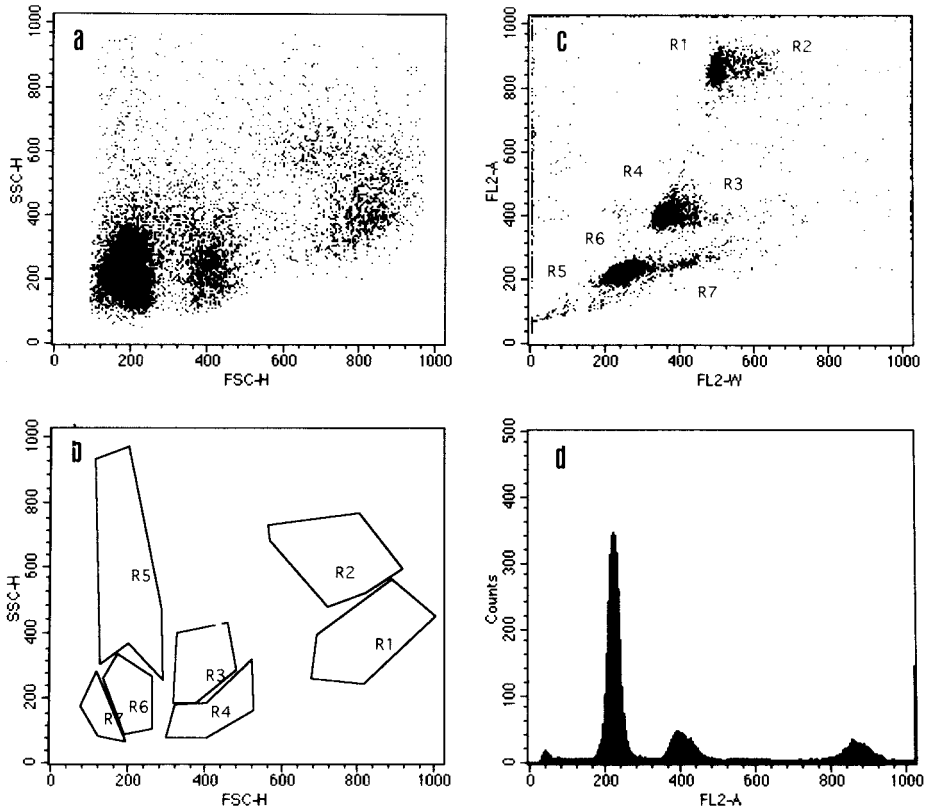

FIG. 2. FACS analysis of a testicular cell suspension obtained from an adult rat. **a**) First window, in which cells are distributed according to size (FSC-H) and cellular granularity (SSC-H). **b**) The frame of the first window overlaid with marks representing the seven gated groups. **c**) Second window, in which cells are distributed according to fluorescence intensity (FL2-A) and width of the emitted fluorescence (FL2-W). Location of gated groups is marked by their group number (R1-R7). **d**) A histogram that represents the number of cells at each fluorescence level.

to the R6+R7 region, and elongated condensed spermatozoa were found in the region determined by gates R5+R6+R7. The fourth and smallest level of fluorescence was emitted by these two latter subpopulations. Identification of the cellular subpopulation within each gate was verified by microscopic examination (Fig. 3, d–f) and by the experiments described below.

To determine the testicular developmental schedule of the rat as compared to that of the mouse by FACS analysis, we followed the development-dependent acquisition pattern of each of the seven subpopulations determined in the mature testis and monitored the percentage of cells with differing DNA content (Table 1). In the mouse (Fig. 4), postnatal (p.n.) Day 7–10 testes exhibited only the two 2d subpopulations (R3 and R4) in the first window. However, in the second and third windows, a small 4d subpopulation (~3%) and a small intermediate subpopulation (~3%), representing cells in S phase of the cell cycle, could be distinguished in addition to the 2d cells (~94%). By p.n. Day 12, a significant number of cells exhibited FSC-H values appropriate for the R1 subpopulation, although they did not appear as a discrete group. At this developmental stage, a significant increase in the portion of 4d cells (~7%, $p < 0.0005$) was observed for the first time (windows 2 and 3). By p.n. Day 14 there was a discrete R1 group, with a further-increased portion of 4d cells (~15%). By p.n. Days 17–18, the R1 group showed very high intensity, with the first indications of R2 cells and with the 4d cells composing ~40% of all cells. Cells localized to the R6 gate were seen for the first time at p.n. Days 20–21 (Fig. 3e) in accordance with the appearance of 1d cells (~7%) in the second and third windows. At this developmental stage the R1 and R2 subpopulations were well established. Elongating spermatids (R7) started to appear at about p.n. Days 24–25, at which time haploid cells composed ~23% of all cells; and by p.n. Days 27–28, elongated spermatozoa were present, as evidenced by the localization of cells to the R5 region and the apparent fourth level of fluorescence intensity. The haploid cells at this developmental stage represented ~75% of all cells.

A similar acquisition pattern for the various testicular subpopulations was obtained with rats, although the pace was slower (Fig. 5). Until p.n. Days 13–14, only cells corresponding to the R3 and R4 regions could be detected in the first window, and the percentage of 4d cells was ~3% for p.n. Day 6 and Day 13. A statistically significant increase in the portion of the 4d cells was obvious for the first time at p.n. Days 17–18 (6%, $p < 0.0005$), although R1 cells, in the first window, could not be determined as a group until p.n. Days 19–20. At this developmental stage,

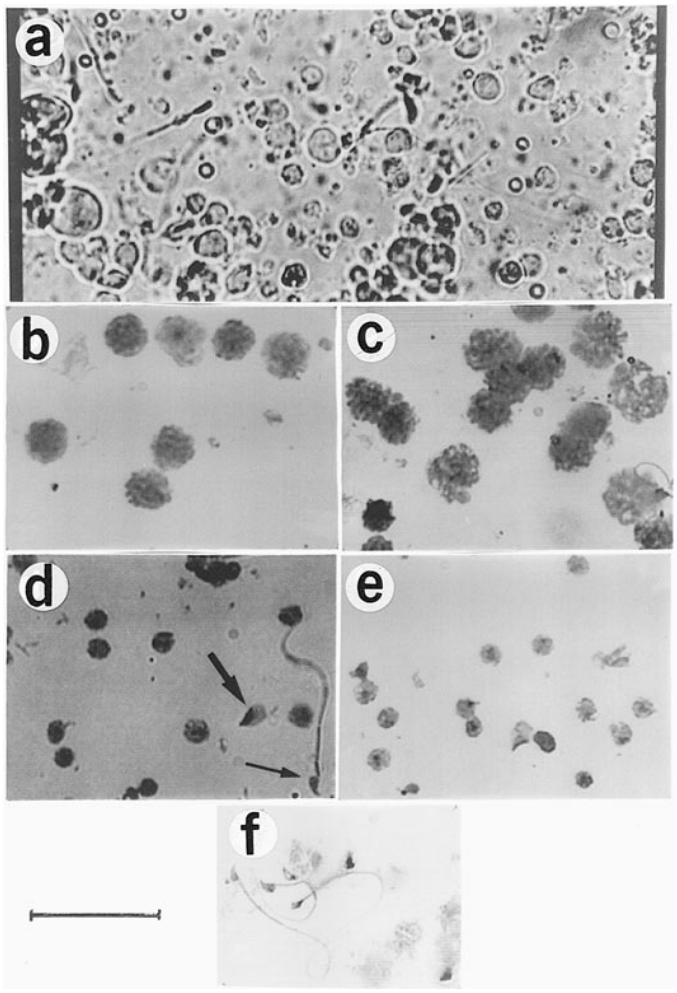

FIG. 3. Light microscopy analysis of various testicular subpopulations. **a**) The testicular cell suspension that was used for FACS analysis. The suspension includes all subpopulations. Cells were not stained. **b**) Cells from subpopulation R1, consisting of primary spermatocytes at the zygotene and early pachytene stages. **c**) Cells from subpopulation R2, consisting of primary spermatocytes at the late pachytene stage. **d**) Cells from subpopulation R6, consisting mainly of early round spermatids, although elongating (thick arrow) and elongated (thin arrow) cells are also included. **e**) Cells from subpopulation R6 of p.n. Day 21 pups. Only round spermatids are present. **f**) Elongated condensed spermatozoa sorted from subpopulation R5. Panels **b–e** show mainly the nuclei of the cells from the specific subpopulations due to treatment with the detergent-containing propidium iodide solution prior to FACS analysis and sorting. Nuclei and cells were stained with hematoxylin. Bar = 50 μm.

TABLE 1. The percentage of 1d, 2d, and 4d cells at the different developmental stages of mouse and rat testes, as determined by FACS analysis in this study.[a]

DNA content of cells[b]	Testicular developmental stage[c]															
	I		II		III		IV		V		VI		VII		VIII	
	M (d7)	R (d6)	M (d10)	R (d13)	M (d12)	R (d17)	M (d14)	R (d20)	M (d17)	R (d22)	M (d21)	R (d24)	M (d24)	R (d30)	M (d27)	R (d36)
1d	0	0	0	0	0	0	0	0	0	0	7	2	23	29	75	65
2d	94	93	94	94	87	91	82	77	44	48	43	49	35	32	9	17
4d	3	3	3	3	7	6	15	19	40	47	46	44	37	33	12	16

[a] Percentage values needed for completion to 100% within each column, represent cells in S-phase and randomly dispersed background cells representing debris, doublets or triplets.

[b] 1d, Haploid cells (one copy of the genome); 2d, diploid cells (two copies of the genome); 4d, diploid cells at the G2 stage of the cell cycle (four copies of the genome).

[c] M, mouse; R, rat; postnatal age in parentheses.

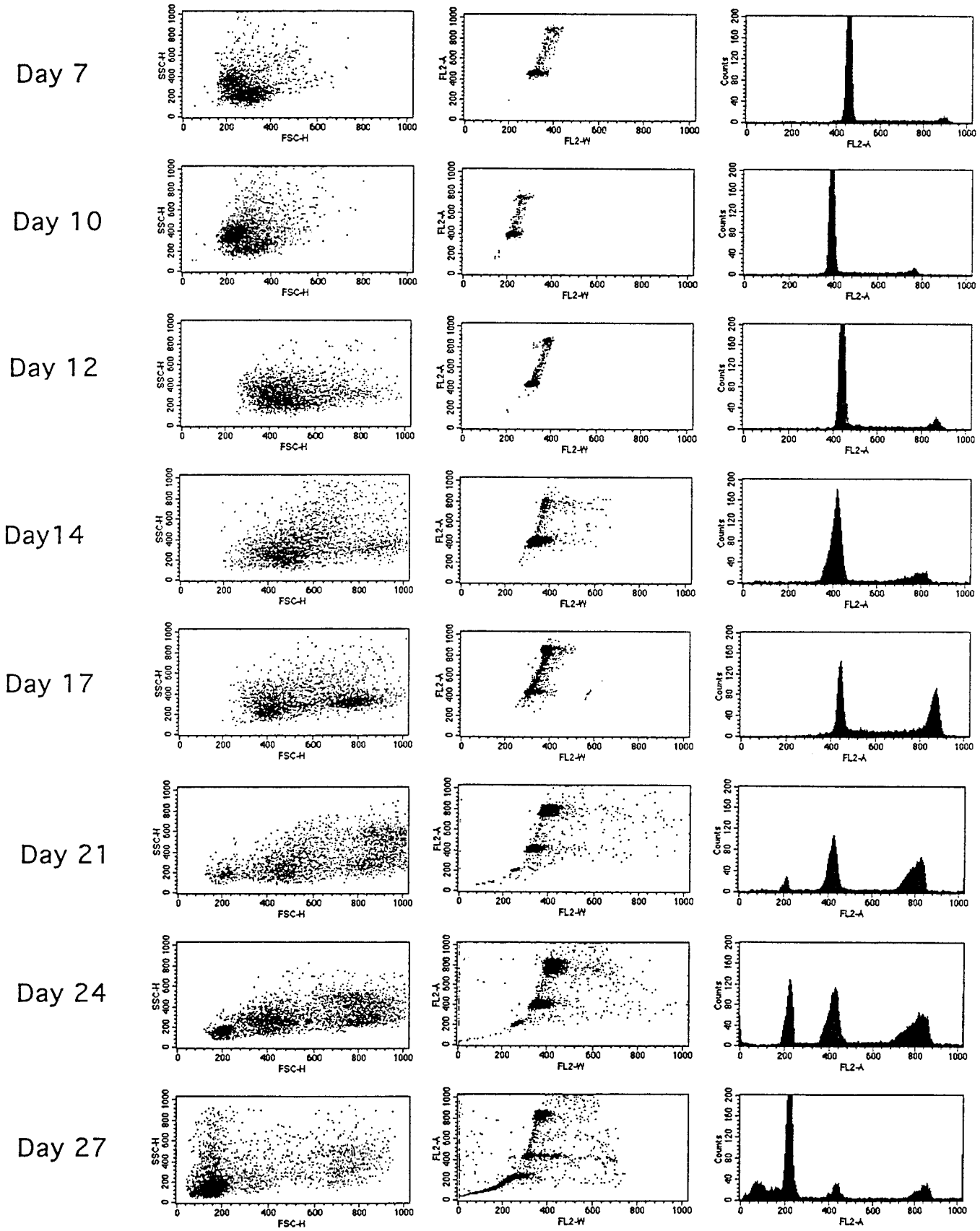

FIG. 4. FACS analysis of a testicular cell suspension obtained from mouse pups at various postnatal developmental stages. All three windows are shown for each developmental stage.

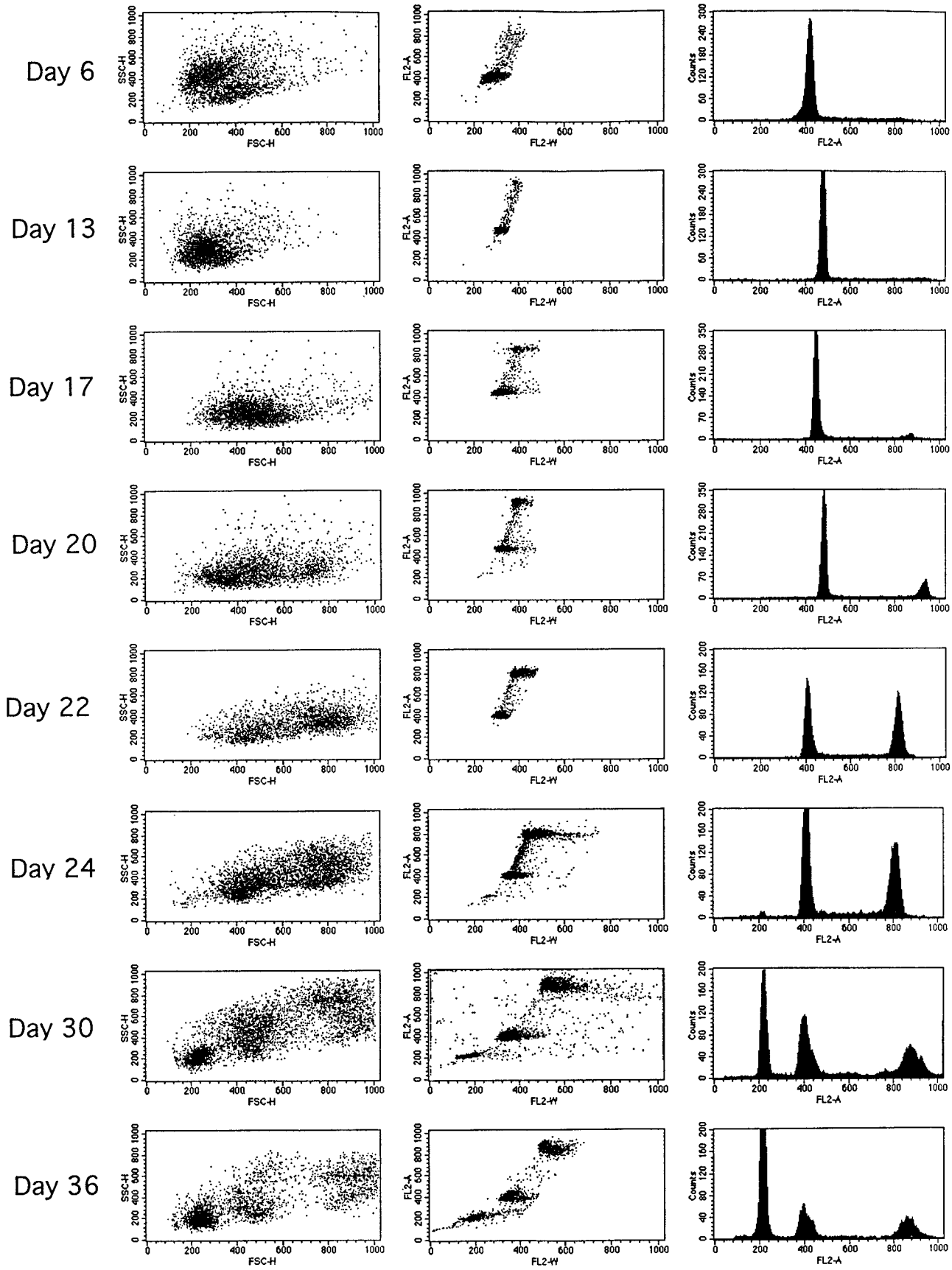

FIG. 5. FACS analysis of a testicular cell suspension obtained from rat pups at various postnatal developmental stages. All three windows are shown for each developmental stage.

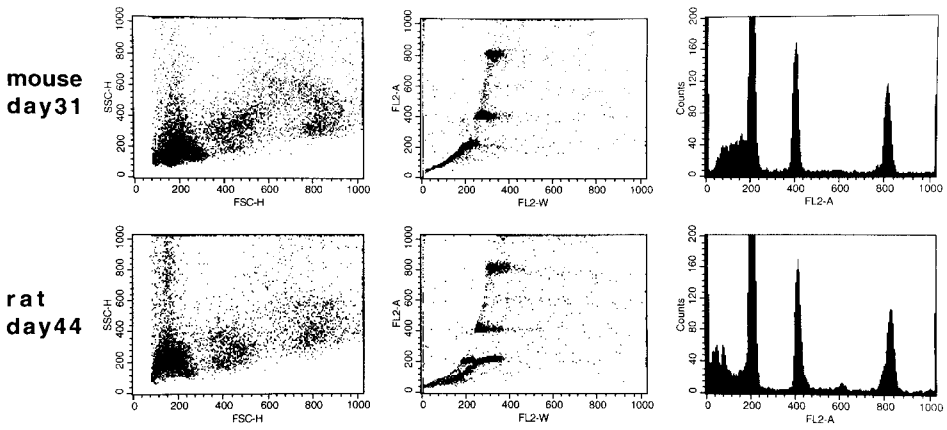

FIG. 6. FACS picture of testicular cells obtained from p.n. Day 31 mouse and p.n. Day 44 rat. Note that all cell subpopulations are present as in the adult.

the 4d cells totaled up to ~19% of all cells (whereas the 2d cells constituted ~77%). By p.n. Days 22–23 it was possible to discriminate between the R1 and R2 subpopulations, and the percentages of the 4d and 2d cells were almost equal, ~47% and ~48%, respectively. The first signs of haploid cells were obtained in all three windows by p.n. Days 24–25 (~2%); and by p.n. Days 30–31, ~29% of the cells in the testicular cell suspension were haploid cells. Of those, a small portion seemed to localize to the R7 region, indicating the presence of elongating spermatids. The smear that defines the R5 region in the FSC-H/SSC-H plot (first window) started to appear at p.n. Days 36–37, indicating that by this developmental stage, the first condensed elongated spermatozoa are present in the testis. This was also evidenced by the appearance of the fourth fluorescence level in the second and third windows. By p.n. Days 42–44, in the rat, the FACS pattern was very similar to that for mature testis (Fig. 6), indicating that the complete spermatogenic complement is present in the seminiferous epithelium at this stage.

DISCUSSION

In this study we used four-parameter flow cytometry to determine the testicular developmental schedule in the rat as compared to that of the mouse. Using the FSC-H/SSC-H parameters, we were able to determine seven distinct subpopulations (R1–R7) that were divided into four major levels of fluorescence (Figs. 1 and 2). The positive correlation between the size of the cells (FSC-H) and the DNA content (FL2-A), demonstrated by the fact that the cells with the highest FSC-H values (R1 and R2) were those containing 4d DNA and that the cells with the intermediate FSC-H values (R3 and R4) were those containing 2d DNA, is in agreement with the results reported by Bellve et al. [23]. The R1 and R2 subpopulations consist of primary spermatocytes that have gone through premeiotic DNA synthesis and have entered meiotic prophase I. Mitotically dividing spermatogonial cells constitute a very small fraction of all adult testicular cells [23], and thus spermatogonial cells at the G2 stage of the cell cycle make a negligible contribution to the 4d population. Somatic cells do not divide in the mature testis [25, 26, 28]. The 2d cells, having intermediate FSC-H values and consisting of somatic cells, secondary spermatocytes, and spermatogonia cells at the G1 stage of the cell cycle (although at a very small proportion, as mentioned above), exhibited two subpopulations based on their SSC-H values (R3 and R4). On the basis of morphological characteristics, we were not able to conclusively associate these two subpopulations with specific testicular cells. Nevertheless, the SSC-H differences between these two subpopulations, which are more apparent in earlier developmental stages, might result from differences in biochemical activities. For example, differences in transcriptional activity (mRNA content) within the 2d cells, as well as within the 4d cells, were reported by Janca et al. [16]. As to the 1d cells in which two peaks of fluorescence were apparent, it has been well documented that fluorescence emitted from haploid cells is distributed within a wide range, with two predominant peaks bordering that range: one representing round spermatids and one representing elongated spermatozoa [11, 14, 19]. This wide fluorescence distribution is a consequence of the chromatin condensation state that dictates propidium iodide intercalation efficiency [15]. Although the haploid cells showed a smeary distribution, we were able to determine three regions, i.e., R5, R6, and R7, by using the FSC-H/SSC-H parameters. All uncondensed round spermatids were concentrated within the R6 region, and elongating spermatids were distributed over the R6+R7 regions, whereas elongated spermatozoa were smeared along R5+R6+R7 regions. This smeary appearance of the elongated cells along the SSC-H axis seems to be a consequence of the orientation of the cells when crossing the laser beam [29].

A flow cytometric follow-up on the development of the postnatal testis has been executed in the past in both the mouse [16] and rat [11]. However, these studies focused on the changes in the DNA content of the cells without further staging within each DNA containing group, especially within the 4d group. Concerning changes in the DNA content, the results reported in the present study on the mouse are in accordance with those of Janca et al. [16]. Regarding rat spermatogenesis, Zhengwei et al. [24] reported that primary spermatocytes first appear on Day 15 and round spermatids on Day 25. Our results are consistent with these findings, although we could not detect a significant increase in the 4d cells until Day 17, since leptotene and early zygotene primary spermatocytes appear prior to the increase in the 4d cells (see discussion below and Table 2). However, there are slight differences between our results and those reported by Clausen et al. [11], especially with regard to the time when haploid cells first appear. These differences might be attributed to the enhanced ability to discriminate signal from background today compared to 20 yr ago.

A morphologically based determination of the mouse testicular developmental schedule was documented by Bellve et al. [23, 30]. According to this developmental schedule,

TABLE 2. The suggested developmental schedule of rat testis compared to that of the mouse.

Stage no.	Description of developmental stage	Age in rat	Age in mouse
I	Spermatogonia and somatic cells only	Days 6–7	Days 6–7
II	Initiation of meiosis I—leptotene cells	Days 13–14	Day 10
III	Appearance of zygotene cells	Days 17–18	Day 12
IV	Appearance of early pachytene cells	Days 19–20	Day 14
V	Appearance of late pachytene cells	Days 22–23	Days 17–18
VI	Appearance of round spermatids	Days 24–25	Days 20–21
VII	Appearance of elongating spermatids	Days 30–31	Days 24–25
VIII	Appearance of elongated spermatozoa	Days 36–37	Days 27–28

seminiferous epithelium from p.n. Day 6 pups contains only primitive type A spermatogonia and Sertoli cells. At p.n. Day 8, type A and type B spermatogonia are present, and by p.n. Day 10, cells from the first spermatogenic wave can be found at preleptotene and leptotene stages of the first meiotic prophase. Zygotene primary spermatocytes are first detected on p.n. Day 12, and early pachytene and late pachytene spermatocytes first appear on p.n. Days 14–15 and Days 17–18, respectively. Haploid round spermatids first appear at about p.n. Day 21, and at about p.n. Day 30 the complete spermatogenic complement is present in the seminiferous epithelium. The results obtained with the mouse in the present study fit this morphologically based developmental schedule and could be divided into eight developmental stages (Fig. 4, Tables 1 and 2). Testes of p.n. Day 6-7 pups (stage I) exhibited 2d cells with few 4d cells, the latter of which consisted of spermatogonia as well as somatic cells at the G2 stage of a mitotic cell cycle. At p.n. Day 10 (stage II), although the FACS pattern seemed unchanged in both the FSC-H and the FL2 parameters, the constant portion of 4d cells (~3%)—despite the greatly reduced frequency of mitotically dividing somatic cells—is consistent with cells of the first spermatogenic wave reaching the leptotene stage of prophase I. There are no R1 cells (in the first window) in this developmental stage, since leptotene spermatocytes are small cells [23]. As the developmental process progresses, more cells from the first spermatogenic wave enter prophase I. As a result, by p.n. Day 12 (stage III), when zygotene cells are first seen, a significant number of cells exhibit FSC-H values appropriate for the R1 subpopulation, although they do not appear as a discrete group. Additionally, a statistically significant increase in the proportion of 4d cells is observed. The progress of cells from the first spermatogenic wave to the early and late pachytene stages (stages IV and V) is characterized by a well-defined R1 group at p.n. Day 14 and acquisition of the R2 subpopulation at p.n. Days 17–18, respectively. Haploid round spermatids first appear (group R6) at p.n. Days 20–21 (stage VI) as expected, and elongating spermatids become apparent by p.n. Days 24–25 (R7, stage VII), whereas elongated condensed spermatids are apparent (R5) from p.n. Day 27–28 (stage VIII). It is noteworthy that although the mouse testicular developmental schedule obtained in the present study is similar to the morphologically based developmental schedule reported by Bellve et al. [23, 30], there is an advantage to determining the FACS pattern of each developmental stage. This enables an efficient separation of the various subpopulations at each developmental stage (with purity more than 90%) and hence analysis of stage-specific events. For example, we were able to obtain a very pure population of early round spermatids from p.n. Day 21 (subpopulation R6, Fig. 3e), whereas in testes of adult mice, this R6 group is ''contaminated'' with elongating and elongated spermatids. It is noteworthy, however, that if intact cells from specific subpopulations are to be obtained by sorting, pretreatment of the cells with a detergent-containing solution (e.g., the propidium iodide solution) is not recommended. That is, sorting according to the FSC-H/SSC-H parameters should be performed without prestaining with a fluorescent dye or, alternatively, with use of a fluorescent dye such as Hoechst 33342 that does not require detergents to penetrate the cells.

In the rat, a very similar acquisition pattern for the various subpopulations, composed of the same eight developmental stages, was found. As in the mouse, rat testis at p.n. Days 6–7 contains only mitotically dividing spermatogonia cells and somatic cells, some of which are still undergoing mitotic divisions. The developmental stage of p.n. Days 13–14 in the rat correlates to p.n. Day 10 in the mouse in the sense that it is the last postnatal age showing no increase in the proportion of 4d cells, although mitotic activity of the somatic cells either ceased [25] or at least dramatically declined [26, 28]. This suggests that, as in the mouse, the rather constant portion of 4d cells is attributable to primary spermatocytes that have entered the leptotene stage of prophase I. The appearance of zygotene cells in the mouse, at p.n. Day 12, was characterized by significant increase in the proportion of 4d cells, for the first time, and by the appearance of a substantial number of cells in the R1 region in the first window. This very exact pattern was found in rats at p.n. Days 17–18, suggesting the first appearance of zygotene cells at that developmental stage. At p.n. Days 19–20, the 4d cells show up as a discrete R1 group for the first time, and by p.n. Days 22–23, a distinct R2 group begins to appear. This correlates to p.n. Day 14 and p.n. Days 17–18 in the mouse, meaning acquisition of early and late pachytene spermatocytes, respectively. Haploid round spermatids were first detected by p.n. Days 24–25, corresponding to p.n. Days 20–21 in the mouse; elongating spermatids started to accumulate by p.n. Days 30–31 (as evidenced by cells that began to occupy the R7 region in the first window), corresponding to p.n. Days 24–25 in the mouse; and rat pups older than 36 days seem to have condensed spermatids in their testes (as evidenced by the first signs of cells within the R5 group), corresponding to pups older than 27–28 days in the mouse. This rat testicular developmental schedule in comparison to that for the mouse is summarized in Table 2. It is noteworthy that the similarity between the rat and mouse along the eight developmental stages is not confined to the flow cytometric picture but includes also the proportion of the various cell types within each developmental stage (Table 1). Nevertheless, the stoichiometry of the various cell types varies among reports ([17, 23, 24] and this study), suggesting that the specific analysis procedure is an important parameter that should first be normalized when quantitative assessment is made. This is important, for example, when FACS

is used to determine the efficiency of spermatogenesis in response to hormonal manipulation.

In conclusion, we believe that identification of the subpopulations that represent the various differentiative stages in the postnatal development of the testis, together with the advantage of sorting and separating each subpopulation with the FACS, gives us a powerful tool for studying mammalian spermatogenesis at the molecular level.

ACKNOWLEDGMENTS

We would like to thank Dr. Ron Wides and Dr. Avi Zusswein for reviewing the manuscript and Mr. Uri Karo for technical assistance.

REFERENCES

1. Kierszenbaum AL. Mammalian spermatogenesis in vivo and in vitro: a partnership of spermatogenic and somatic cell lineages. Endocr Rev 1994; 15:116–134.
2. Haqq CM, King CY, Donahoe PK, Weiss MA. SRY recognizes conserved DNA sites in sex-specific promoters. Proc Natl Acad Sci USA 1993; 90:1097–1101.
3. Nishimune Y, Okabe M. Mammalian male gametogenesis: growth, differentiation and maturation of germ cells. Dev Growth Differ 1993; 35:479–486.
4. Hecht NB, Bower PA, Waters SH, Yelick PC, Distel RJ. Evidence for haploid expression of mouse testicular genes. Exp Cell Res 1986; 164: 183–190.
5. Kleene KC, Flynn JF. Characterization of a cDNA clone encoding a basic protein, TP2, involved in chromatin condensation during spermiogenesis in the mouse. J Biol Chem 1987; 262:17272–17277.
6. Shih DM, Kleen KC. A study by in situ hybridization of the stage of appearance and disappearance of the transition protein 2 and the mitochondrial capsule seleno-protein mRNAs during spermatogenesis in the mouse. Mol Reprod Dev 1992; 33:222–227.
7. Unni E, Meistrich ML. Purification and characterization of the rat spermatid basic nuclear protein TP4. J Biol Chem 1992; 267:25359–25363.
8. Romrell LJ, Bellve AR, Fawcett DW. Separation of mouse spermatogenic cells by sedimentation velocity. A morphological characterization. Dev Biol 1976; 49:119–131.
9. Meistrich ML. Separation of spermatogenic cells and nuclei from rodent testes. Methods Cell Biol 1977; 15:15–54.
10. Wolgemuth DJ, Gizang-Ginsberg E, Englemyer E, Gavin BJ, Ponzetto C. Separation of mouse testis cells on a Celsep TM apparatus and their usefulness as a source of high molecular weight DNA or RNA. Gamete Res 1985; 12:1–10.
11. Clausen OPF, Purvis K, Hansson V. Application of micro flow fluorometry to studies of meiosis in the male rat. Biol Reprod 1977; 17: 555–560.
12. Grogan WM, Farnham WF, Sabau JM. DNA analysis and sorting of viable mouse testis cells. J Histochem Cytochem 1981; 29:738–746.
13. Clausen OPF, Parvinen M, Kirkhus B. Stage related variations in DNA fluorescence distribution during rat spermatogenic cycle measured by flow cytometry. Cytometry 1982; 2:421–425.
14. Van Kroonenburgh MJ, Beck JL, Scholtz JW, Hacker-Klom U, Herman CJ. DNA analysis and sorting of rat testis cells using two parameter flow cytometry. Cytometry 1985; 6:321–326.
15. Evenson D, Darzynkiewicz Z, Jost L, Janca F, Ballachey B. Changes in accessibility of DNA to various fluorochromes during spermatogenesis. Cytometry 1986; 7:45–53.
16. Janca FC, Jost LK, Evenson DP. Mouse testicular and sperm cell development characterized from birth to adulthood by dual parameter flow cytometry. Biol Reprod 1986; 34:613–623.
17. Rosiepen G, Weinbauer GF, Schlatt S, Behre HM, Nieschlag E. Duration of the cycle of the seminiferous epithelium, estimated by the 5-bromodeoxyuridine technique, in laboratory and feral rates. J Reprod Fertil 1994; 100:299–306.
18. Weinbauer GF, Limberger A, Behre HM, Nieschlag S. Can testosterone alone maintain the gonadotrophin-releasing hormone antagonist-induced suppression of spermatogenesis in the non-human primate. J Endocrinol 1994; 142:485–495.
19. Petit MJ, Ratinaud MH, Cordelli E, Spano M, Julien R. Mouse testis cell sorting according to DNA and mitochondrial changes during spermatogenesis. Cytometry 1995; 19:304–312.
20. Fossa SD, Slide J, Theodorsen L, Pettersen EO. Pre-treatment DNA ploidy of sperm cells as a predictive parameter of post treatment spermatogenesis in patients with testicular cancer. Br J Urol 1994; 74: 359–365.
21. Hittmair A, Rogatsch H, Mikuz G, Feichtinger H. Quantification of spermatogenesis by dual-parameter flow cytometry. Fertil Steril 1994; 61:746–750.
22. Heidenrich A, Zunbe J, Engelmann UH. Diagnosis and follow-up of testicular carcinoma in situ by DNA image cytometry. Eur Urol 1995; 28:13–18.
23. Bellve AR, Cavicchia CJ, Millette CF, O'brien DA, Bhatnagar YM, Dym M. Spermatogenic cells of the prepuberal mouse: isolation and morphological characterization. J Cell Biol 1977; 74:68–85.
24. Zhengwei Y, Wreford NG, de Kretser DM. A quantitative study of spermatogenesis in the developing rat testis. Biol Reprod 1990; 43: 629–635.
25. Steinberger A, Steinberger E, Replication pattern of Sertoli cells in maturing rat testis in vivo and in organ culture. Biol Reprod 1971; 4: 84–87.
26. Orth JM. Proliferation of Sertoli cells in fetal and post-natal rats: a quantitative autoradiographic study. Anat Rec 1982; 203:485–492.
27. Bellve AR, Feig LA. Cell proliferation in the mammalian testis: biology of the seminiferous growth factor (SGF). Recent Prog Horm Res 1984; 40:531–567.
28. Nagy F. Cell division kinetics and DNA synthesis in the immature Sertoli cells of the rat testis. J Reprod Fertil 1972; 28:389–395.
29. Spano M, Evenson DP. Flow cytometric analysis for reproductive biology. Biol Cell 1993; 78:53–62.
30. Bellve AR, Millette CF, Bhatnagar YM, O'brien DA. Dissociation of the mouse testis and characterization of isolated spermatogenic cells. J Histochem Cytochem 1977; 25:480–494.